Electronic Supplementary Material (ESI) for Environmental Science: Atmospheres.

Supplement of

Performance of Vehicle Add-On Mobile Monitoring System $PM_{2.5}$ Measurements During Wildland Fire Episodes

Ashley S. Bittner et al.

Correspondence to: Ashley Bittner (bittner.ashley@epa.gov)

S1 Details of Vehicle Add-On Mobile Monitoring System

The VAMMS mobile PM monitor is self-contained in a crush-proof case (Figure S1) designed to be operated in any vehicle. VAMMS data is formatted for use with EPA's Real Time Geospatial Data Viewer (RETIGO - https://www.epa.gov/hesc/real-time-geospatial-data-viewer-retigo). RETIGO is an online app that the VAMMS operator can upload VAMMS data to for automatic generation of maps and timeseries of measurement data. The VAMMS is easiest to operate in the passenger or back passenger seat immediately next to a window to allow the sample probe to be installed on the window (Figure S2).

Figure S1: The VAMMS package contains the following components: PM monitor (pDR-1500, Thermo Scientific), GPS (Ultimate GPS Breakout, Adafruit), data logger, local SD card data storage, lithium-ion battery (12V 45 W), sampling probe and window mount with sample tubing and GPS antenna, 120V AC power cord, auxiliary car power cord, zero check HEPA filter, and spare 37 mm filter for PM collection.

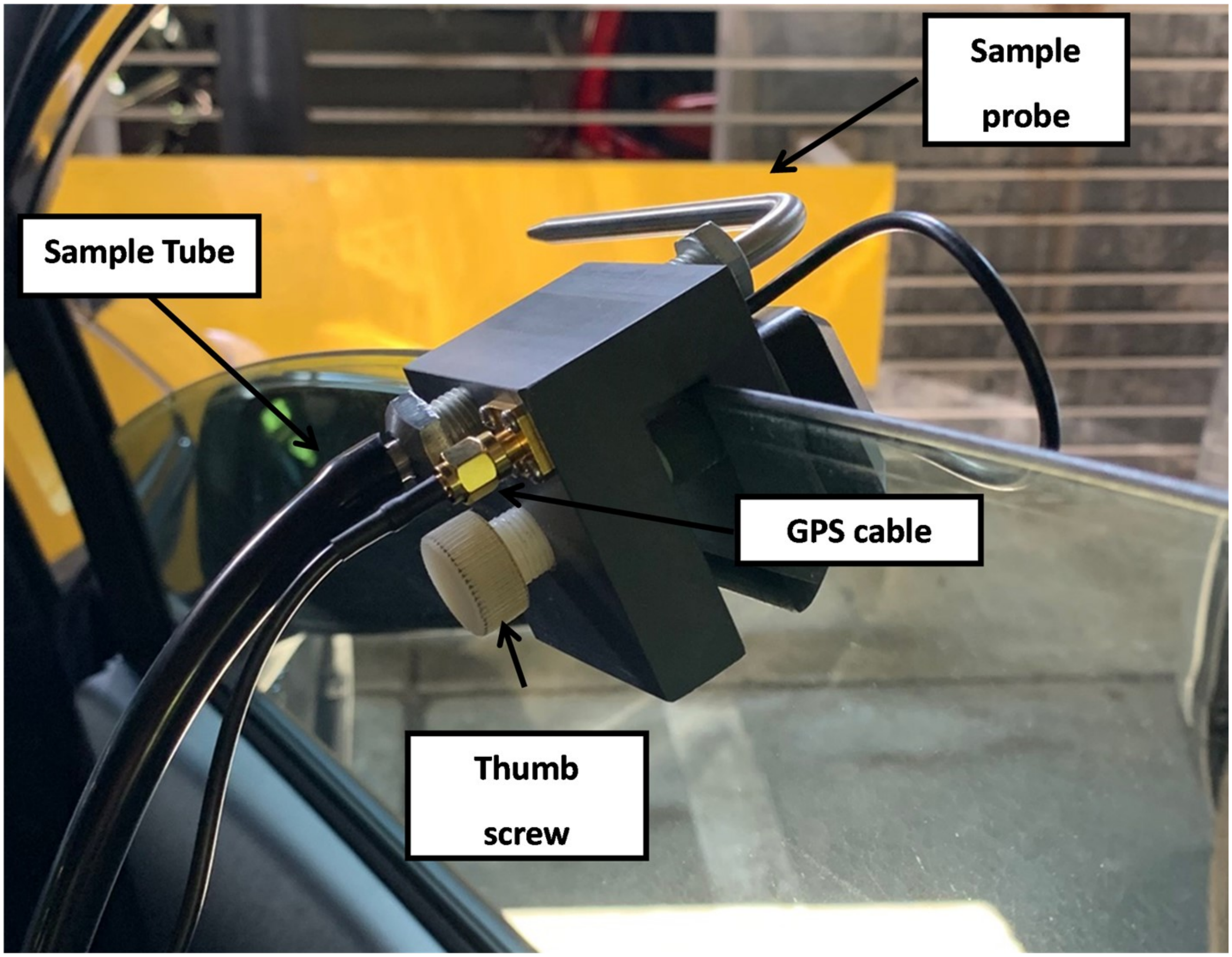

Figure S2: The sampling configuration of the VAMMS on the passenger window of a vehicle. The sample probe is connected to the sample tube, which connects to an inlet on the exterior of the VAMMS case. An interior tube connects the sample tube to the pDR-1500. The GPS cable is also attached to its own inlet on the VAMMS case. The probe faces forward into the airstream to sample PM as the VAMMS is driving. The thumbscrew is used to tighten the mount in place.

We determined the isokinetic sampling vehicle velocity for this probe to be approximately 35 mph using the following approach:

$$v_{probe} = \frac{Q}{A} = \frac{Q}{\pi R^2} = \frac{5.833 * 10^{-5} \frac{m^3}{s}}{\pi \left(1.065 * 10^{-3}\, m\right)^2}$$

$$= 16.37\ m/s = 36.6\ MPH \approx 35\ MPH$$

where Q is the sampling flow rate (3.5 LPM), and R is the radius of the probe inlet (D/2 = 0.084”/2).

Faster or slower sampling velocities can result in anisokinetic sampling conditions which impact how particles are quantified. To explore this effect on our data sets, we first determined the median driving speed for each campaign (Table S1).

Table S1: Median and mean (± standard deviation) driving speed (mph) for each field data collection campaign: Cedar Creek wildfire (OR), Monument wildfire (CA), and Konza Prairie prescribed burns (KS). The Konza Prairie data were collected using an all-terrain vehicle on non-road terrain, so the driving speeds were much lower than the wildfire samples which were collected using on-road vehicles on traditional roadways and highways.

	Median speed (mph)	Mean speed ± sd (mph)
Cedar Creek	38.9	37 ± 27
Monument	31.1	30 ± 26
Konza Prairie	5.6	6.6 ± 5.3

At higher velocities (e.g., Cedar Creek), sampling is subisokinetic (probe velocity < vehicle velocity) which leads to over-sampling of high-inertia coarse particles. Conversely at slower velocities (e.g., Konza Prairie), sampling is superisokinetic (probe velocity > vehicle velocity) leading to an over-sampling of low-inertia fine particles[1]. To quantify the mass error, we first used the Particle Loss Calculator Tool[2] to estimate sampling efficiency (i.e., how efficiently aerosol particles are drawn into the described probe) across a range of particle sizes from 0.01 to 5 µm at the median velocity for each of our data collection campaigns (Figure S3).

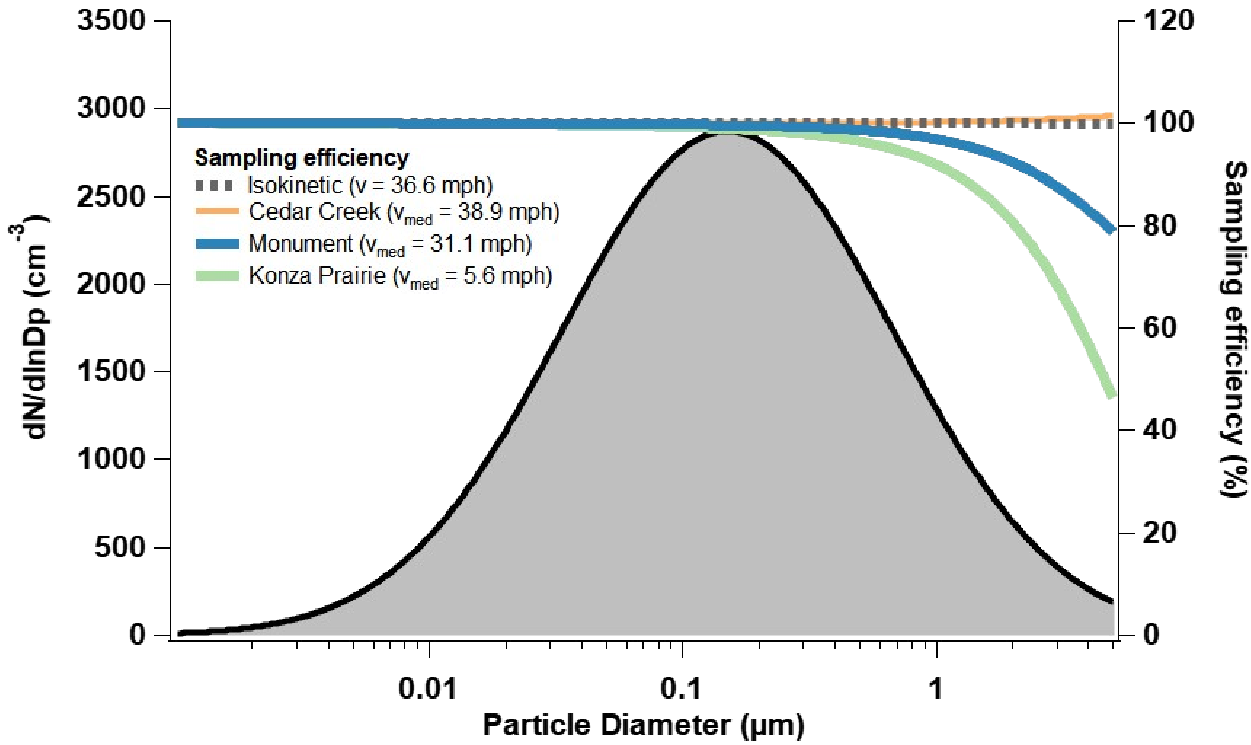

Figure S3: Simulated particle size distribution (N=5400, geometric mean diameter = 200 µm, geometric standard deviation = 1.5)[1] as a function of particle diameter (µm) for aerosol typical of biomass combustion. The sampling efficiency (%) at each particle diameter for the median sampling velocity for each field dataset (Cedar Creek, Monument, Konza Prairie) is given on the right axis. Isokinetic or ideal sampling is shown as the black dotted line. The median velocity is given in parenthesis in the figure legend. At efficiencies greater than 100%, more large aerosol particles are drawn inside the sampling tube than were originally included in the sampling volume, and efficiencies less than 100% describes the opposite. Sampling efficiency source: Particle Loss Calculator Tool[2].

Many studies have shown that biomass aerosol is mostly submicron in size and can be unimodal or bimodal with a geometric mean diameter of ~150 nm and a geometric standard deviation around 1.5 for aged aerosol[3–7]. We generated a simulated particle size distribution (PSD) using these parameters reflective of biomass burning aerosol (Figure S3). There are few particles above 1 micron, but they account for most of the mass (Figure S4).

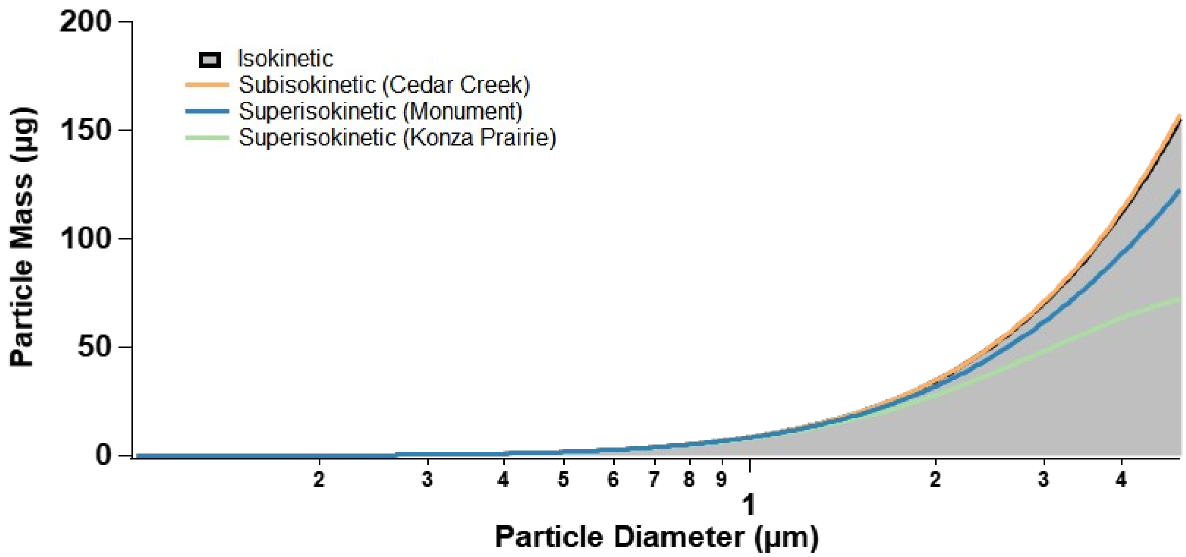

Figure S4: Particle mass (µg) versus particle diameter (µm) calculated from the simulated biomass burning aerosol particle size distribution assuming spherical particles of uniform density. The ideal or true mass is shown in grey, measured isokinetically. The colored lines show the mass that would be measured given sub- and superisokinetic sampling conditions for each of three datasets (estimated using the median sampling velocity).

We convolved the simulated PSD with the sampling efficiency at each particle diameter to estimate the percent error in the summed $PM_{2.5}$ (particulate matter less than 2.5 microns) mass measurement for each field dataset (Table S2). For the Cedar Creek dataset, we found that anisokinetic sampling would result in a negligible bias (or overestimate) of 0.47% for the $PM_{2.5}$ mass measurement. The impact on the Monument dataset was slightly larger but still modest (-6.3%). The impact on the Konza Prairie data set was more significant, resulting -16.2% bias, implying that the VAMMS likely underestimated the true mass concentration.

Table S2: Sampling efficiency (η) at 0.1, 1 and 2.5 micrometers determined using the Particle Loss Calculator Tool[2] at isokinetic sampling velocity and the median velocity observed during the three field data set used in this analysis. The total $PM_{2.5}$ mass (µg), based off the simulated particle size distribution, that would be measured by each campaign (given the sampling efficiency) is shown and was used to calculate the estimated mass bias (%).

	η at 0.1 µm	η at 1 µm	η at 2.5 µm	$PM_{2.5}$ mass (µg)	$PM_{2.5}$ bias (%)
Isokinetic	1.000	1.000	1.000	3173	
Cedar Creek	1.000	1.002	1.007	3188	+ 0.47
Monument Fire	0.997	0.969	0.900	2972	-6.3
Konza Prairie	0.992	0.919	0.746	2660	-16.2

S2 Details of source subtraction method

We estimated the vehicle velocity with the latitude, longitude, and timestamp data using the Haversine distance function which determines the great-circle distance between two points on a sphere. The calculated distance (and thus velocity) is only an approximation as this assumes the Earth to be a perfect sphere. The Haversine (or great circle) distance is given by:

$$D(x,y) = 2\arcsin[\sqrt{\sin^2((x1-y1)/2) + \cos(x1)\cos(y1)\sin^2((x2-y2)/2)}] \quad \text{(Eqn 0)}$$

Where x1 is the starting latitude, x2 is the ending latitude, y1 is the starting longitude, and y2 is the ending longitude.

A running coefficient of variation (COV) method[8] was used to identify dust spikes in the $PM_{2.5}$ concentration data likely attributable to acceleration of the vehicle on pavement, gravel, or dirt. According to Brantley et al. (2014)[9]:

"The COV method consists of calculating the rolling 5 s standard deviation (2 s before and after the center data point) and dividing it by the mean concentration of the sampling run. The 99th percentile of the calculated COV is used as a threshold and any data points with a COV above this threshold are flagged along with the data points 2 s before and after."

We used the raw 1-s data for source subtraction and the 99th percentile to identify and remove dust spikes. As a secondary check, we visually inspected each timeseries before and after source subtraction using the coincident velocity timeseries to assess if flagged spikes were related to vehicle acceleration and not an actual source (see Figure S5 for an example). Using this approach, we adjusted the percentile to the 99.5th (instead of 99th) in two sampling runs (out of 33 total considered for this paper) where it appeared too much data were flagged for removal. Two sampling runs were not included in the analysis because the vehicle was stationary for more than 25% of the run. A table of percentiles and threshold values for each sampling run is given in Table S3. The threshold value ranged between 0.01 and 1.5 depending on the data set.

This procedure flagged < 1% of data on average with most of the flagged events occurring just after velocity increased or decreased rapidly (Figure S5). The flagged data points were excluded from the $PM_{2.5}$ concentration data for a given sampling run. In this paper, we consider a sampling run to be a single-day VAMMS deployment event. If the user stopped sampling for a few hours and resumed within the same day, we considered this to be the same sampling run.

Table S3: The percentile, COV threshold, and percentage of data removed for each sampling run included in this analysis. The event for each file is also given.

Date	Percentile	Threshold	Data removed (%)	Event
8/11/2021	99	0.06	1.00	Monument Fire
8/13/2021	99	0.06	1.00	
8/14/2021	99	0.05	1.00	
8/15/2021	99	0.07	1.00	
8/16/2021	99	0.04	1.00	
8/17/2021	99.5	0.10	0.50	
8/19/2021	99.5	0.12	0.50	
8/20/2021	99	0.22	1.00	
8/21/2021*	99	0.39	1.00	
8/24/2021	99	0.18	1.00	
8/25/2021	99	0.28	1.00	
8/26/2021*	99	0.29	1.00	
8/27/2021	99	0.07	1.00	
8/28/2021	99	0.14	1.00	
8/29/2021	99	0.05	1.00	
9/1/2021	99	0.08	1.00	
9/6/2021	99	0.15	1.00	
9/13/2021	99	0.03	1.00	
9/14/2021	99	0.06	1.00	
9/16/2021	99	0.11	1.00	
9/18/2021	99	0.15	1.00	
9/19/2021	99	0.42	1.00	
9/24/2022	99	0.45	1.00	Cedar Creek Fire
9/25/2022	99	0.26	1.00	
9/26/2022	99	0.23	1.00	
9/27/2022	99	0.13	1.00	
9/29/2022	99	0.38	1.00	
9/30/2022	99	0.41	1.00	
10/3/2022	99	0.56	1.00	
10/4/2022	99	0.41	1.00	
10/7/2022	99	0.39	1.00	
10/8/2022	99	0.36	1.00	
10/10/2022	99	0.15	1.00	
10/12/2022	99	0.14	1.00	
9/15/2021	99	1.49	1.00	Konza
median	**99.00**	**0.15**	**1.00**	
mean	**99.03**	**0.24**	**0.97**	
minimum	**99.00**	**0.03**	**0.50**	
maximum	**99.50**	**1.49**	**1.00**	

* Data from these days were excluded from analysis because the vehicle was not moving for a large portion of the run.

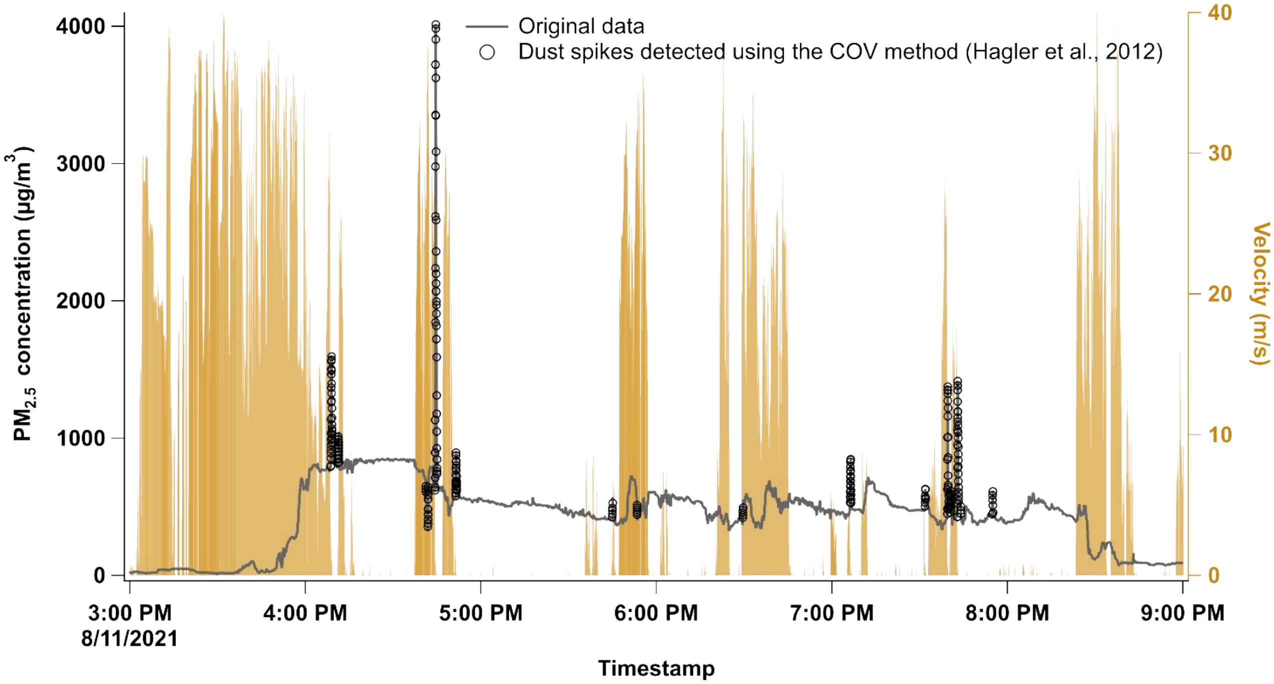

Figure S5: Example of dust spikes (resulting from vehicle acceleration on pavement) detected in the $PM_{2.5}$ concentration data and removed using the COV method[8]. The velocity is shown on the right-hand axis in meters per second. These data were collected near Shasta-Trinity County, CA during the Monument Fire on 08/11/2021. The timestamp is given in Universal Coordinated Time.

S3 Details of instrument corrections

VAMMS

For each VAMMS deployment, we compared the mean concentration from the corrected pDR-1500 to the blank-corrected, filter-derived concentration determined via gravimetric analysis (Figure S6). To account for mass gained or lost during handling and quality assurance checks, we subtracted the mean value of the six blank filters (-0.0191 mg) from each deployment filter before calculating the filter-derived concentration using the total sampling duration and flow values. A net mass loss in this range is consistent with handling, relative humidity, and temperature effects for blank glass fiber filters[10].

We did not correct the real-time pDR-1500 values using the gravimetric filter mass from each deployment. During deployment, VAMMS data are interpreted immediately after collection by the ARA to conduct time-sensitive analysis and response activities, rather than retroactively. In emergency response mode, users are not able to compare or correct the real-time pDR-1500 measurements to the integrated filter mass concentration. For this reason, we only show data with the Delp and Singer (2020)[11] correction in the text.

For the Cedar Creek fire, the mean pDR-1500 concentration was 30% higher than the concentration derived from the filter. We suspect that the Delp and Singer correction[11], applied indiscriminately to all pDR-1500 data, may explain this difference. Road dust, which would have a different mass scattering efficiency than wildfire PM, would not be suitable for correction by the Delp and Singer equation[11], potentially skewing the pDR-1500 mean concentration too high when impacted by dust. This impact would be most noticeable for the longer, on-road deployments, like the Cedar Creek or Monument fires, though we do not have a filter for the Monument fire to confirm.

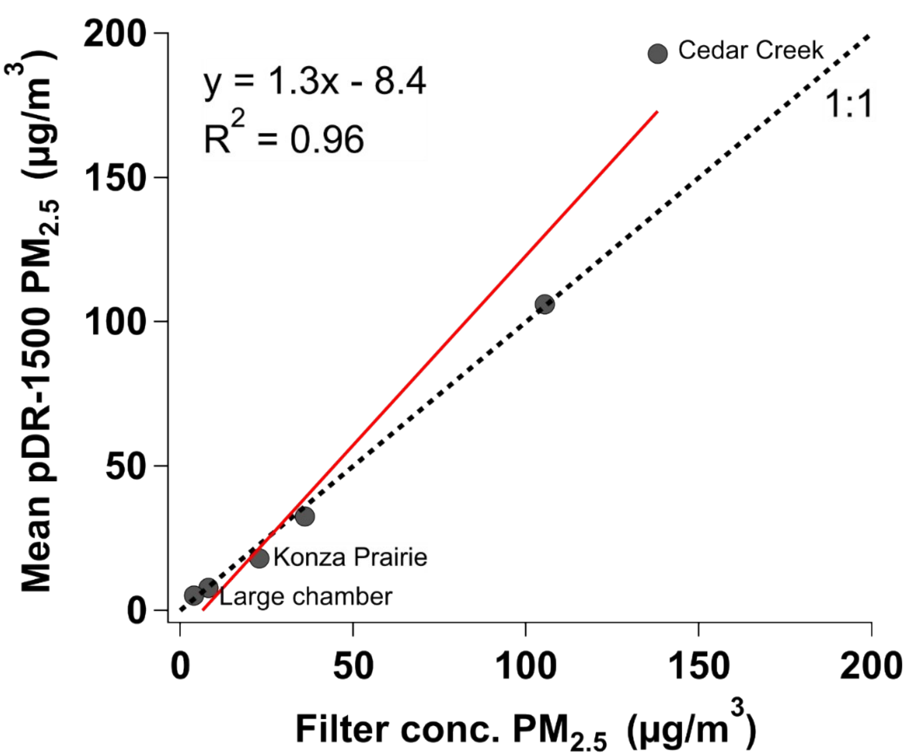

Figure S6: The mean pDR-1500 $PM_{2.5}$ concentration versus the concentration derived from the blank-corrected integrated filter mass for six deployments. Text labels are only given for deployments included in this analysis. Linear fit regression coefficients (red line) and the R^2 value are shown. A one-to-one line is shown as the dotted black line.

PurpleAir

Using the collocated instruments at the Oakridge AQMS, we compared the performance of uncorrected PurpleAir data and data corrected using two wildfire-specific literature corrections to the on-site FEM during the Cedar Creek fire. We compared uncorrected raw data and data corrected using two smoke-specific correction factors to each other and to nearby reference monitors during both wildfires. The corrections were developed for wildfire smoke conditions using wildland fire smoke-impacted data from the Western U.S[12,13]. The form of the first correction equation from Barkjohn et al. (2022)[12] is piecewise quadratic:

PAcf1 < 570 (corrected = 300 μg/m3 at 50% RH):

$$PM_{2.5} = PAcf1 \times 0.524 - 0.0862 \times RH + 5.75 \quad (1)$$

570 ≤ PAcf1 < 611:

$$PM_{2.5} = (0.0244 \times PAcf1 - 13.9) \times [\text{Equation (3)}] + (1 - (0.0244 \times PAcf1 - 13.9)) \times [\text{Equation (1)}] \quad (2)$$

PAcf1 ≥ 611 (corrected 400 μg/m3):

$$PM_{2.5} = PAcf1^2 \times 4.21 \times 10{-}4 + PAcf1 \times 0.392 + 3.44 \quad (3)$$

Where 'PAcf1' is the raw cf=1 value from the A and B channels, 'RH' is the relative humidity measured by the PurpleAir, and $PM_{2.5}$ is the corrected concentration value. The form of the second equation from Holder et al. (2020)[13] is linear:

$$PM_{2.5} = -3.21 + 0.51 \times PAcf1 \quad (4)$$

During the Cedar Creek fire, for the 18 days spanning the VAMMS monitoring period, we compared 1-hr averaged uncorrected and corrected measurements (N=501) from the five PurpleAir monitors to the regulatory monitor located at the Oakridge air quality monitoring station (Figure S7). Uncorrected PurpleAir data and data corrected using the extreme wildfire correction[12] overestimated concentrations relative to the BAM-1022 (Figure S7). PurpleAir data corrected using the wildfire smoke correction[13] showed the best performance.

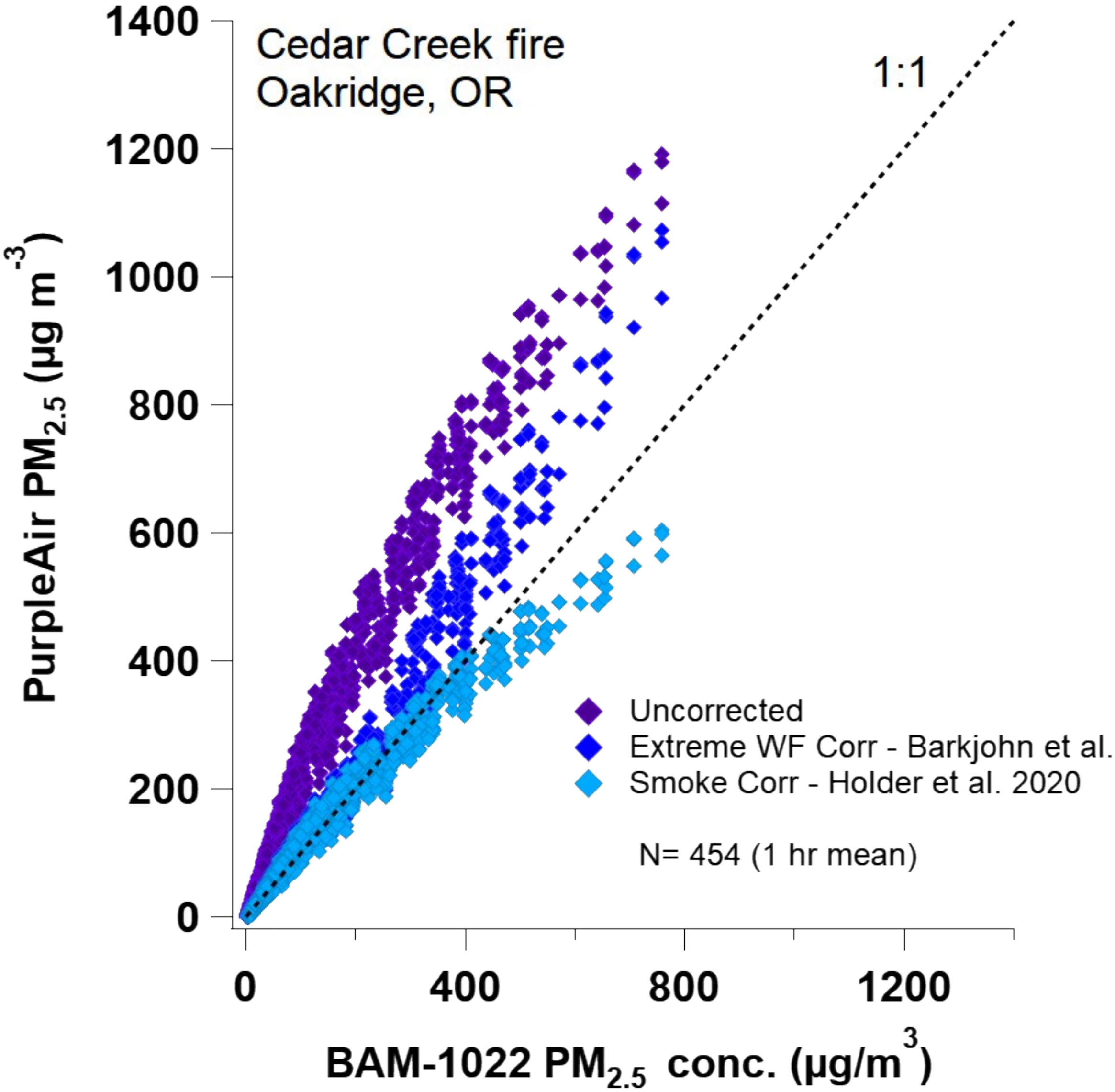

Figure S7: PurpleAir $PM_{2.5}$ concentration (uncorrected, corrected by extreme wildfire correction – Barkjohn et al. (2022)[12], and corrected by wildfire smoke correction – Holder et al. (2020)[13] from three sensors (y-axis) versus the $PM_{2.5}$ concentration measured by the on-site BAM-1022 FEM instrument (x-axis). N is the number data points for each sensor. A one-to-one line is shown as a black dotted line. The data were collected between 09/24/2022 and 10/13/2022 in Oakridge, Oregon during the Cedar Creek wildfire.

Performance statistics for each smoke-corrected PurpleAir are shown in Table S4. All three sensors met the target ranges[14] for all metrics except for intercept. The PurpleAir had high precision between the three instruments (COV < 5%) and all showed high linearity with minimal bias and moderate error. All but one PurpleAir ('Oakridge 2') underestimated the BAM-1022 (slope < 1) concentration. The impact of this was most notable at concentrations above 600 µg m^{-3}. This suggests that at higher time resolutions (10-min), PurpleAir data will underestimate peak concentrations. For the remaining analysis, we used only the 'best' of the three PurpleAir to compare to the VAMMS, 'Oakridge 1', which had the lowest RMSE.

Table S4: Performance statistics from the three PurpleAir (corrected with Holder et al. (2020) smoke-correction) compared to the FEM BAM-1022 monitor at the Oakridge AQMS. Data were 1-hr averaged. R^2 = coefficient of determination, slope and intercept are the fit coefficients from a linear regression, RMSE = root mean square error, and NRMSE = normalized root mean square error.

	Oakridge 1	**Oakridge 2**	**Oakridge 3**
R^2	0.98	0.98	0.98
Slope	0.98	1.09	0.85
Intercept	12.4	8.2	12.2
RMSE	21.4	26.6	28.6
NRMSE	0.16	0.22	0.24

Additionally, we looked at uncorrected and smoke corrected PurpleAir data during the Monument wildfire using the FEM datasets and the nearest PurpleAir sensor, which supported the findings from the Cedar Creek comparison (Figure S8). Notably, the two AQMS and the nearest PurpleAir were farther apart in the Monument fire comparison (150 m and 3 km). Further, at the Weaverville AQMS, hourly ambient $PM_{2.5}$ concentrations regularly exceeded 600 µg m^{-3}, up to 1000 µg m^{-3}. During these periods (approximately three measurement days), the smoke corrected PurpleAir data underestimated the true concentration.

A list of all PurpleAir sensors included in Monument fire analysis is given in Table S5. For Figure S8a, we used data from the BAM-1020 stationed at the Weaverville AQMS and a PurpleAir located approximately 150 m away at the Trinity County library (PA1). For Figure S8b, we used data from the BAM-1022 stationed at the Redding AQMS and a PurpleAir located approximately 3 km away at the Shasta County Health & Human Services Agency (PA17).

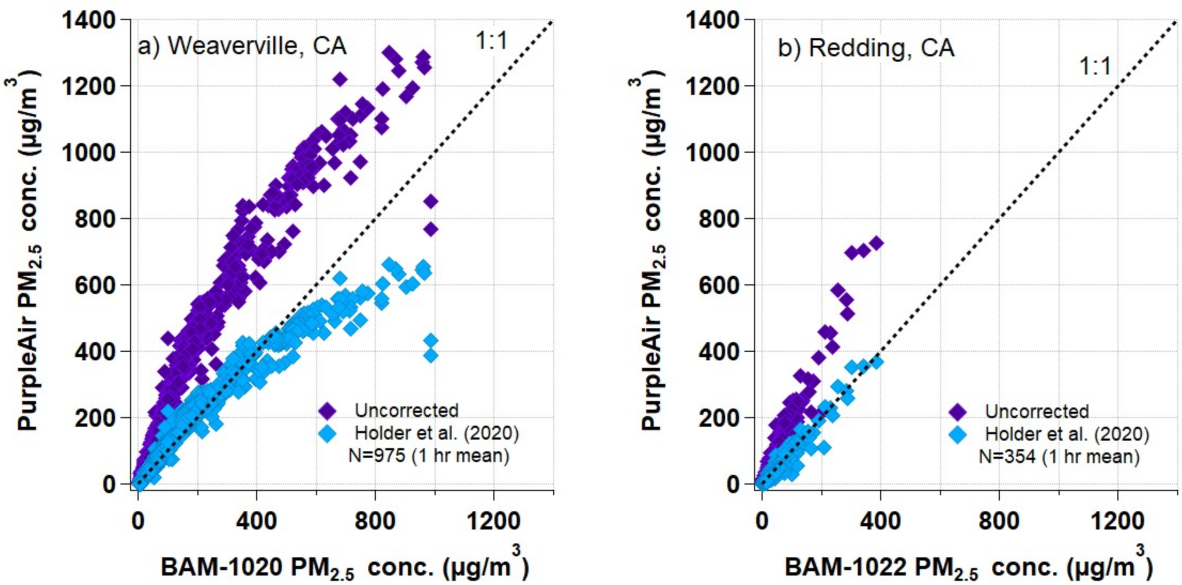

Figure S8: PurpleAir $PM_{2.5}$ concentration (uncorrected and corrected by wildfire smoke correction – Holder et al. (2020)[13] from a PurpleAir sensor versus the $PM_{2.5}$ concentration measured by the on-site FEM instrument (x-axis) for the (a) Weaverville AQMS and (b) Redding AQMS. N is the number data points. A one-to-one line is shown as a black dotted line. The data were collected between 08/10/2021 and 09/20/2021 near Shasta Trinity County during the Monument wildfire.

Table S5: GPS coordinates, ID number, name, N = number of data points (2-min averaged) during which VAMMS passed within range, and mean distance from the VAMMS (in meters) for those passages for each of the twenty-seven PurpleAir sensors included in the Monument wildfire analysis. Data were obtained through the Remote Sensing Information Gateway Application Programming Interface (API) using an API key available through PurpleAir, Inc.

	Longitude	Latitude	ID	Name	N	Distance (m)
PA1	-122.9424	40.7355	40001	NC#119 Weaverville Library	236	150
PA2	-122.3895	40.5962	7308	Alder Gardens	9	115
PA3	-122.3744	40.5894	8038	SHASTAAQMD-TURTLEBAYFORESTCAMP	11	315
PA4	-122.3854	40.8900	8112	SHASTAAQMD_LAKEHEADVOLFIRE	2	130
PA5	-122.3234	40.7549	13039	Bridge Bay at Shasta Lake	3	117
PA6	-122.4904	40.6097	19989	Rock Creek	5	950
PA7	-122.9656	40.3635	55243	Harrison Gulch	5	25
PA8	-122.3919	40.5806	57493	Gerlinger Steel & Supply	62	730
PA9	-122.8062	40.6980	7976	NC#75_Lewiston	48	1000
PA10	-122.3958	40.5802	8058	CARB_SMOKE_SHASTAAQMD_AQMDOFFICE	76	90
PA11	-122.5932	40.6511	85907	Whiskeytown NRA - Oak Bottom Fire Station	16	95
PA12	-122.3820	40.6162	103902	Kennys Air	5	600
PA13	-122.9779	40.6341	107906	B-Bar-K	25	1700
PA14	-122.8065	40.7072	13803	Deadwood	24	65
PA15	-122.7969	40.3176	13737	McFarland ICP – Platina	39	120
PA16	-122.3665	40.6008	63133	Nancy's Air	7	500
PA17	-122.3510	40.5582	8116	SHASTAAQMD_ENTERPRISEEHSSQUAD	6	500
PA18	-122.3444	40.5684	96061	Foxtail Ct Research Center	13	670
PA19	-122.3920	40.5991	35745	Del Mar Ave	4	600
PA20	-122.4095	40.5882	96923	ShastaAQMD_SC2_ShastaHS	29	225
PA21	-122.9437	40.7312	118981	Wood shed	14	415
PA22	-122.9368	40.7272	109050	CATC-OD	125	50
PA23	-122.3720	40.5894	109958	TB-SS sensor	31	475
PA24	-122.4051	40.5537	112622	Sungold Circle	1	620
PA25	-122.4295	40.5888	112920	Sunday	16	575
PA26	-123.0562	40.7242	13817	Junction City	56	400
PA27	-123.1651	40.5526	36685	NC#121_USFS Shasta-Trinity	69	40

Ambilabs nephelometer

Since the Ambilabs nephelometer was corrected to the on-site BAM 1022 monitor, consequently, the 1-hr averaged data from the nephelometer was nearly identical to the 1-hr BAM 1022 data (R^2 = 1, slope = 1, intercept = 0 μg m^{-3}, RMSE = 0.03 μg m^{-3}).

S4 AQI $PM_{2.5}$ Category Definitions

Table S6: Air Quality Index color, category name, and corresponding $PM_{2.5}$ concentration limits.

Category Colors	Category Names	$PM_{2.5}$ Concentration Limits ($\mu g\ m^{-3}$)
Green	Good	0 – 12.0
Yellow	Moderate	12.1 – 35.4
Orange	Unhealthy for sensitive groups	35.5 – 55.4
Red	Unhealthy	55.5 – 150.4
Purple	Very unhealthy	150.5 – 250.4
Maroon	Hazardous	250.5 – 500.4
Gray	Beyond AQI	≥ 500.5

S5 Details of Cedar Creek fire

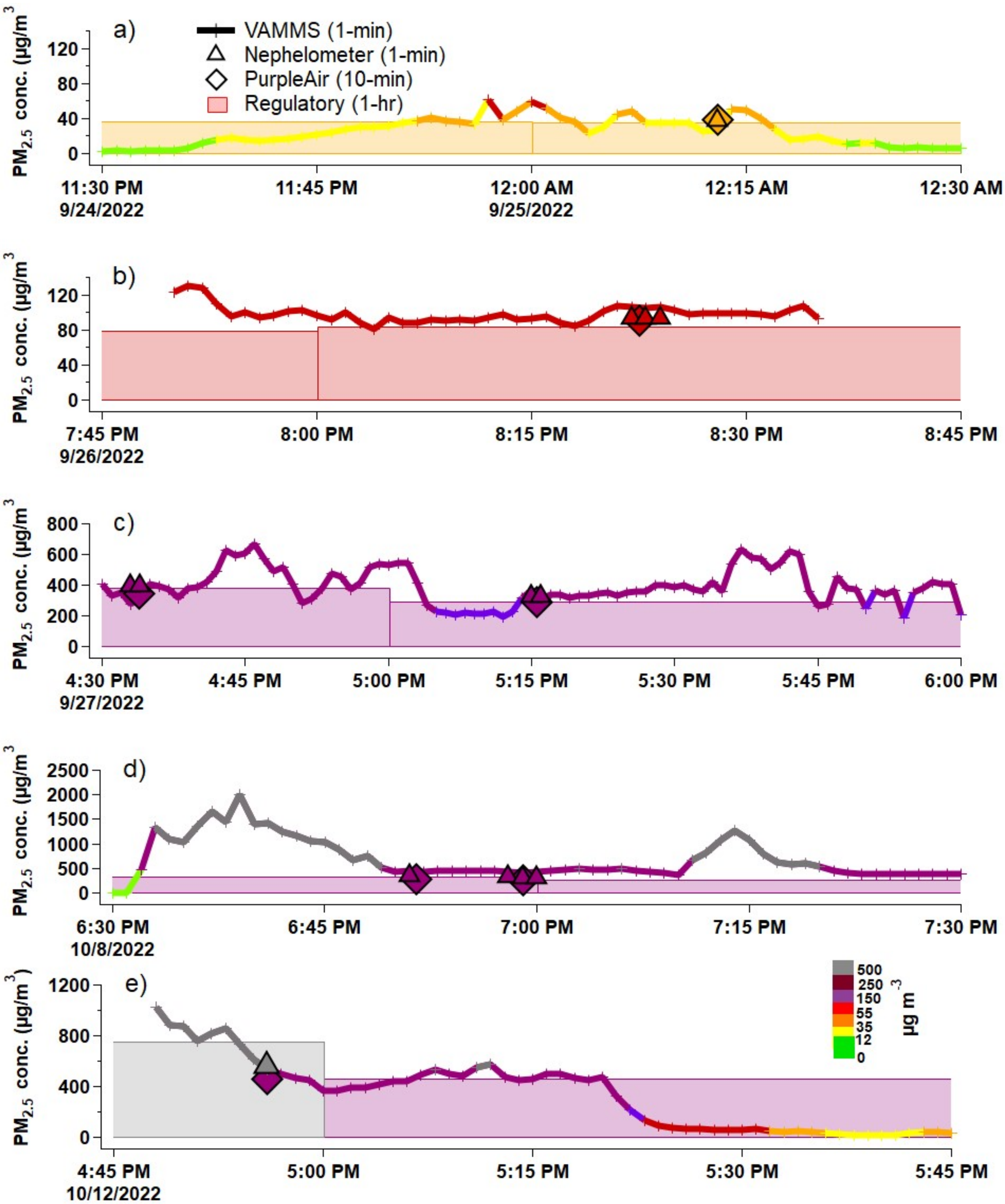

Figure S9: Timeseries of VAMMS (1-min), nephelometer (1-min), PurpleAir (10-min), and BAM 1022 (60-min) $PM_{2.5}$ measurements at the Oakridge, OR air quality monitoring station during the Cedar Creek fire, colored by the corresponding approximate AQI category. Data from the nephelometer and PurpleAir are shown only when the VAMMS was within 400 m of them. The timestamp is given in Universal Coordinated Time.

S6 Details of Konza Prairie prescribed burns

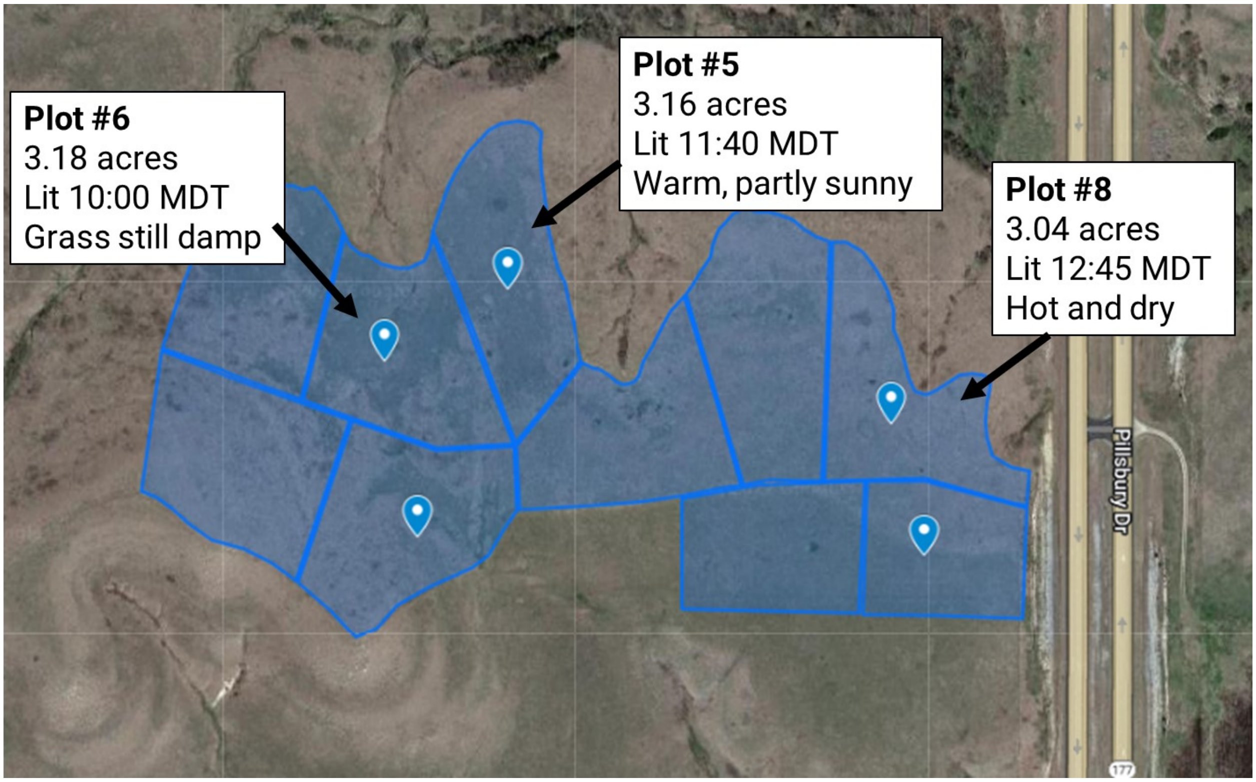

Figure S10: Map of Konza Prairie Biological Research Station near Manhattan, Kansas. The blue regions indicate different plots and the lines between them represent fire breaks. The blue markers indicate the five plots that were burned during the 2-day monitoring period. The three plots burned on 09/15/2021 (day 2) are indicated with arrows and text labels which provide information on the plot size, start time of each burn and the conditions. Google My Maps. Manhattan, Kansas, USA. Accessed: November 17, 2022. © **Google Maps 2022.**

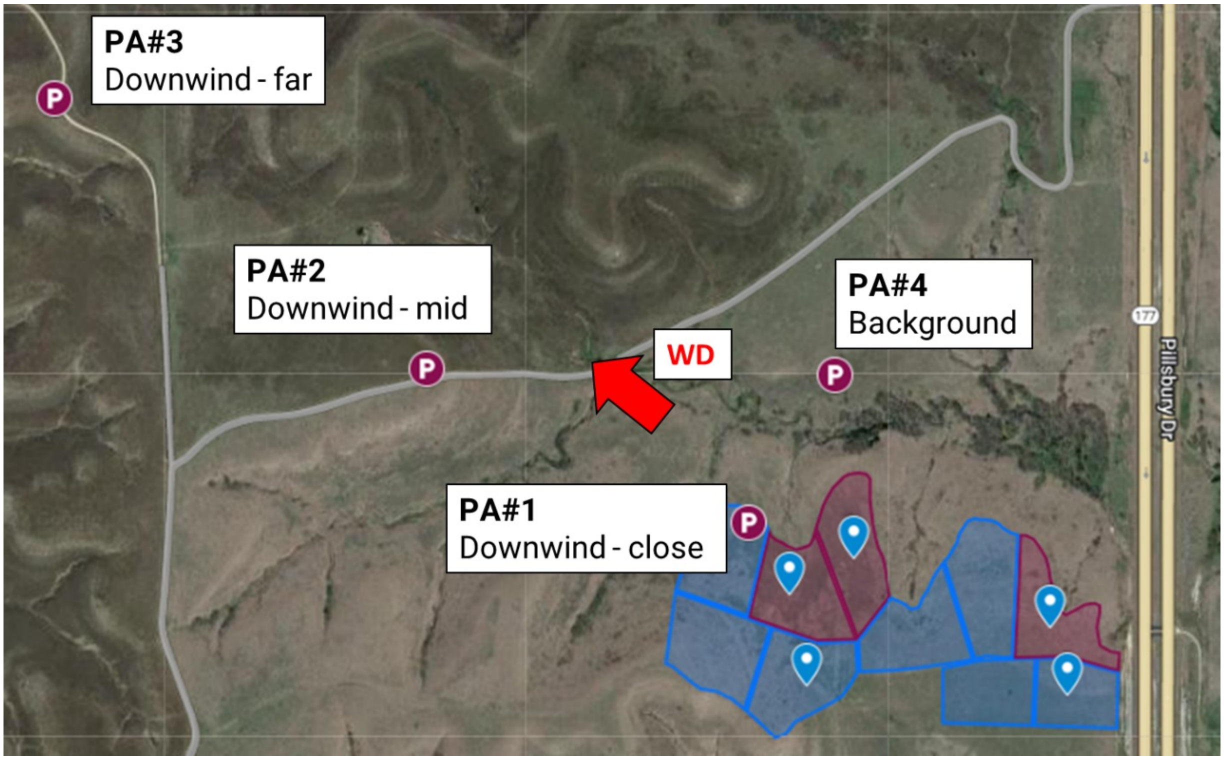

Figure S11: Map of Konza Prairie Biological Research Station near Manhattan, Kansas. The blue regions indicate different plots and the lines between them represent fire breaks. The blue markers indicate the five plots that were burned during the 2-day monitoring period. The three plots burned on 09/15/2021 (day 2) are indicated in maroon. The locations of the four PurpleAir (PA) sensors are indicated with maroon "P" icons. The PurpleAir are numbered and labelled with a description of their approximate location compared to the plots. The red arrow indicates the primary wind direction (WD) during the burns. Google My Maps. Manhattan, Kansas, USA. Accessed: November 17, 2022. **© Google Maps 2022.**

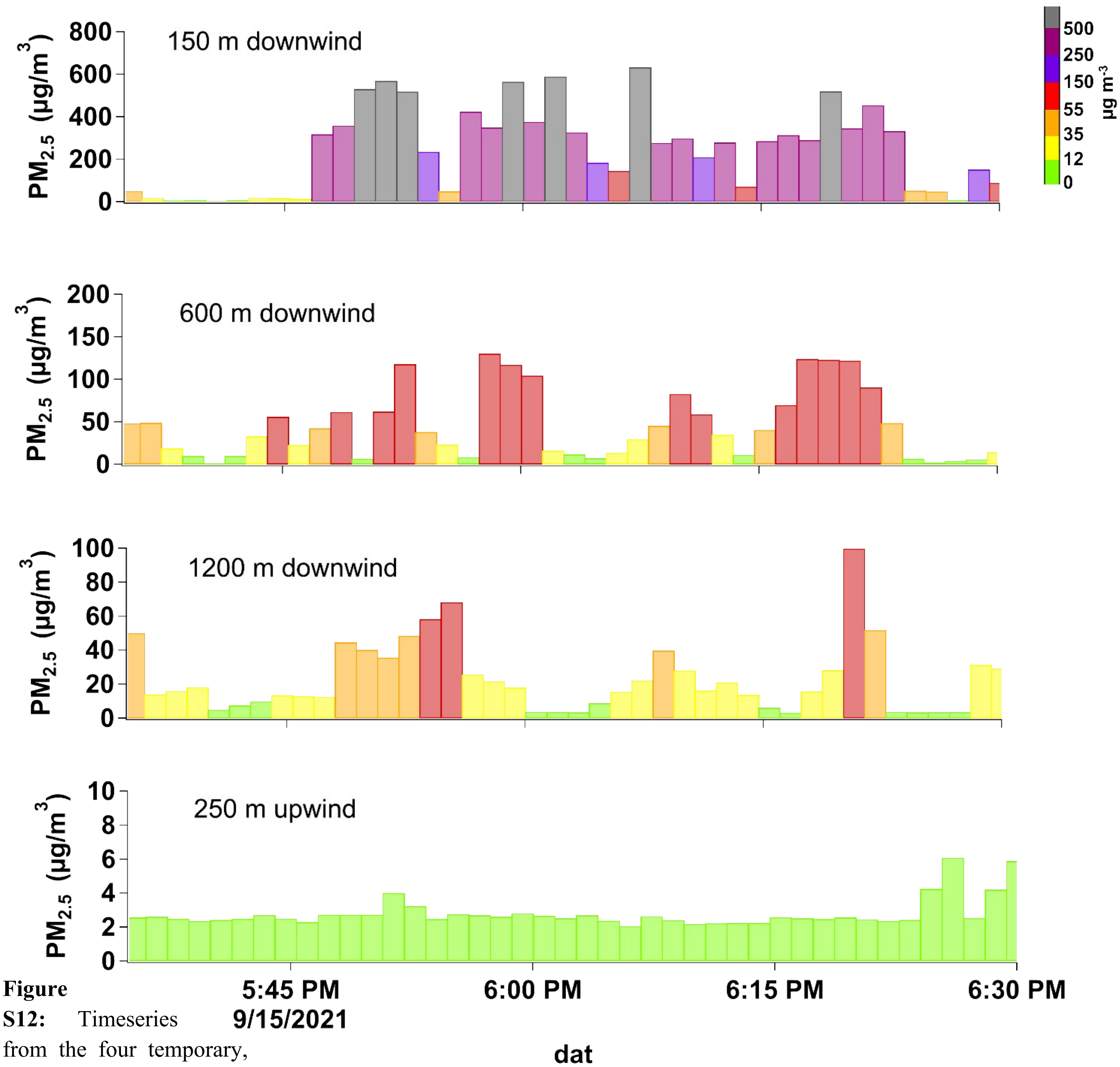

Figure S12: Timeseries from the four temporary, stationary PurpleAir sensors during one 3-acre controlled burn at the Konza Prairie Biological Research Station on 09/15/2021. Each bar represents an 80-s measurement, colored by the 'approximate AQI' concentration. Three sensors were deployed at different distances downwind of the plots (a-c) and one sensor was deployed upwind to record the background concentration (d). The timestamp is given in Universal Coordinated Time.

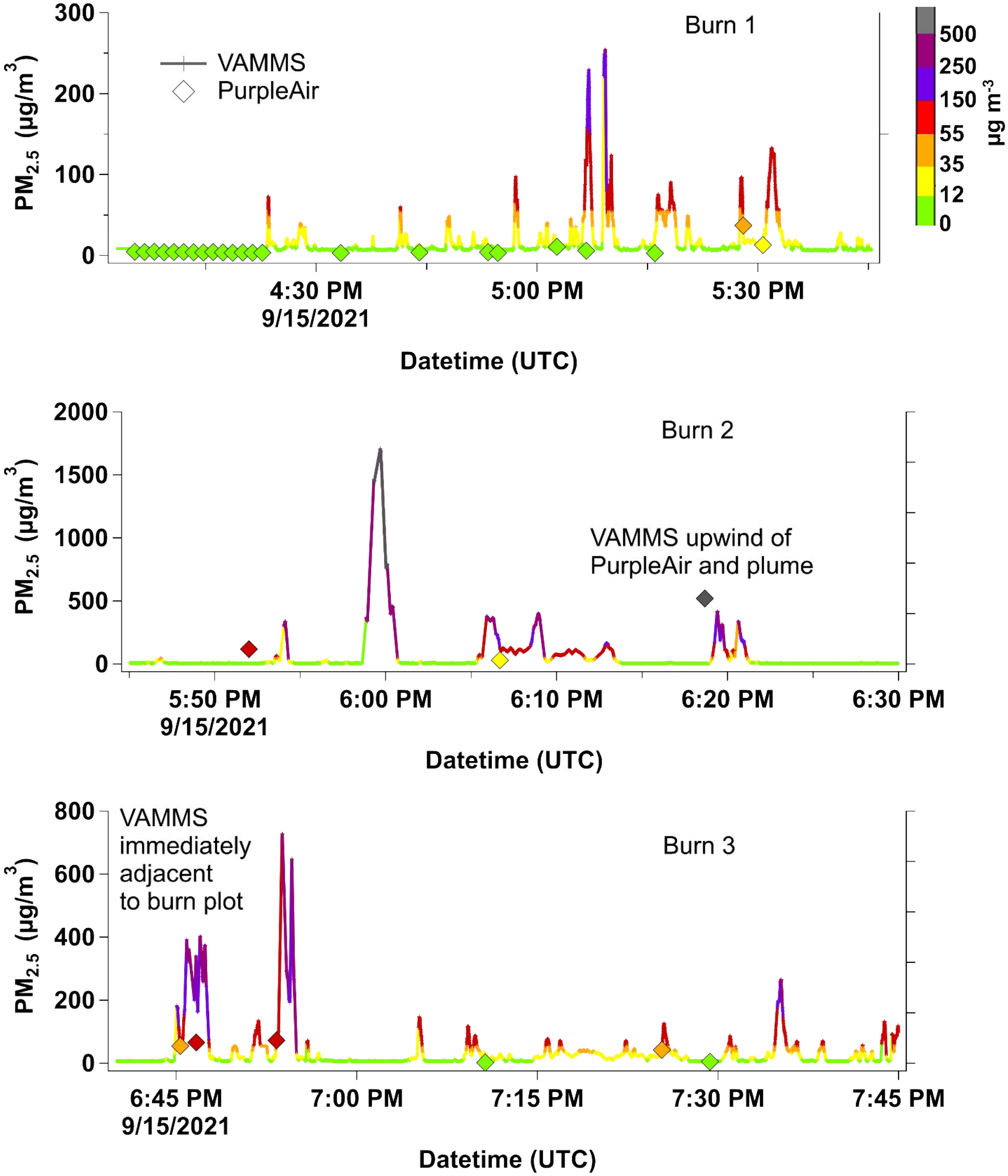

Figure S13: Timeseries of VAMMS (1-s) and PurpleAir (80-s) measurements during prescribed burning on 09/15/2021. Each panel shows the timeseries for the controlled burn of one 3-acre plot. Data from the PurpleAir are shown only when the VAMMS was within 100 m of the instruments. The timestamp is in Universal Coordinated Time.

Figure S14: Image of plume from mid-downwind location (PurpleAir #2). An example of wind conditions lofting the plume above and out of the valley.

Figure S15: Image of plume from near upwind (PurpleAir #4) location. The downwind – close (PurpleAir #1) and downwind – mid (PurpleAir #2) locations are also indicated. An example of the wind conditions causing the plume to fumigate the valley.

S7 Details of high-time resolution measurements

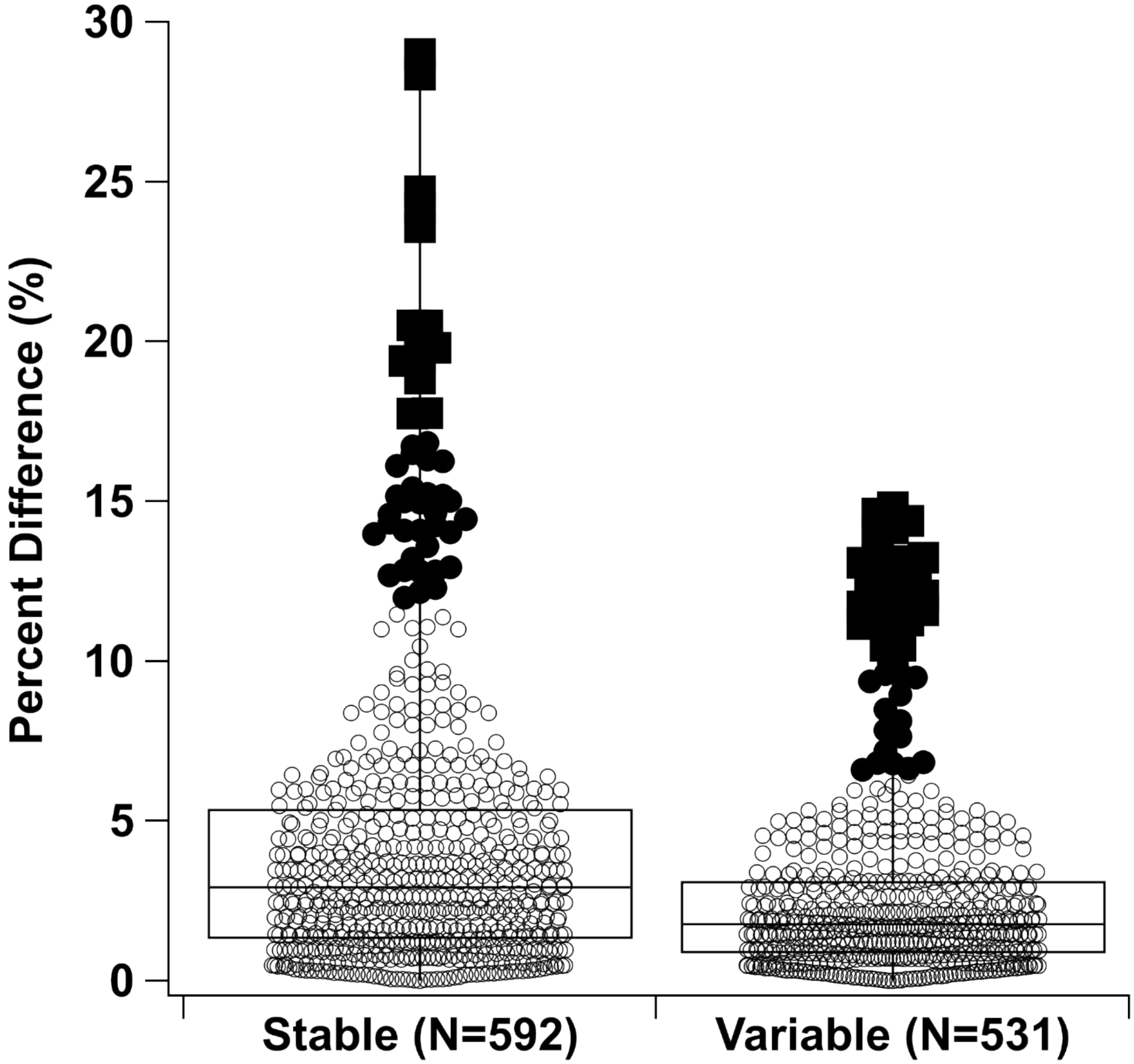

Figure S16: Box plots of the percent difference of the 1-s VAMMS concentration measurement compared to the 1-min mean VAMMS measurements for 'stable' and 'variable' conditions identified during the Cedar Creek fire analysis (Section 3.4) For the Tukey boxplots, the median is the line, the top and bottom of the box are the 75th and 25th quartiles, the whiskers are the minimum and maximum value. Outliers (1.5 * interquartile range) are shown as dark circles and far outliers (3 * interquartile range) as dark squares. These data were collected between 09/25/2022 and 10/12/2022 during the Cedar Creek wildfire near Oakridge, OR.

References

(1) Hinds, W. C. *Aerosol Technology: Properties, Behavior, and Measurement of Airborne Particles, Edition 2*; John Wiley & Sons: Hoboken, NJ, 1999.

(2) Von Der Weiden, S.-L.; Drewnick, F.; Borrmann, S. Particle Loss Calculator – a New Software Tool for the Assessment of the Performance of Aerosol Inlet Systems. *Atmos. Meas. Tech.* **2009**, *2* (2), 479–494. https://doi.org/10.5194/amt-2-479-2009.

(3) Laing, J. R.; Jaffe, D. A.; Hee, J. R. Physical and Optical Properties of Aged Biomass Burning Aerosol from Wildfires in Siberia and the Western USA at the Mt. Bachelor Observatory. *Atmos. Chem. Phys.* **2016**, *16* (23), 15185–15197. https://doi.org/10.5194/acp-16-15185-2016.

(4) Shirman, T.; Shirman, E.; Liu, S. Evaluation of Filtration Efficiency of Various Filter Media in Addressing Wildfire Smoke in Indoor Environments: Importance of Particle Size and Composition. *Atmosphere* **2023**, *14* (12), 1729. https://doi.org/10.3390/atmos14121729.

(5) Reid, J. S.; Koppmann, R.; Eck, T. F.; Eleuterio, D. P. A Review of Biomass Burning Emissions Part II: Intensive Physical Properties of Biomass Burning Particles. *Atmos. Chem. Phys.* **2005**, *5* (3), 799–825. https://doi.org/10.5194/acp-5-799-2005.

(6) Liu, Y.; Meng, X.; Wu, Z.; Huang, D.; Wang, H.; Chen, J.; Chen, J.; Zong, T.; Fang, X.; Tan, T.; Zhao, G.; Chen, S.; Zeng, L.; Guo, S.; Huang, X.; He, L.; Zeng, L.; Hu, M. The Particle Phase State during the Biomass Burning Events. *Science of The Total Environment* **2021**, *792*, 148035. https://doi.org/10.1016/j.scitotenv.2021.148035.

(7) Sakamoto, K. M.; Allan, J. D.; Coe, H.; Taylor, J. W.; Duck, T. J.; Pierce, J. R. Aged Boreal Biomass-Burning Aerosol Size Distributions from BORTAS 2011. *Atmos. Chem. Phys.* **2015**, *15* (4), 1633–1646. https://doi.org/10.5194/acp-15-1633-2015.

(8) Hagler, G. S. W.; Lin, M.-Y.; Khlystov, A.; Baldauf, R. W.; Isakov, V.; Faircloth, J.; Jackson, L. E. Field Investigation of Roadside Vegetative and Structural Barrier Impact on Near-Road Ultrafine Particle Concentrations under a Variety of Wind Conditions. *Science of The Total Environment* **2012**, *419*, 7–15. https://doi.org/10.1016/j.scitotenv.2011.12.002.

(9) Brantley, H. L.; Hagler, G. S. W.; Kimbrough, E. S.; Williams, R. W.; Mukerjee, S.; Neas, L. M. Mobile Air Monitoring Data-Processing Strategies and Effects on Spatial Air Pollution Trends. *Atmospheric Measurement Techniques* **2014**, *7* (7), 2169–2183. https://doi.org/10.5194/amt-7-2169-2014.

(10) Brown, A. S.; Yardley, R. E.; Quincey, P. G.; Butterfield, D. M. Studies of the Effect of Humidity and Other Factors on Some Different Filter Materials Used for Gravimetric Measurements of Ambient Particulate Matter. *Atmospheric Environment* **2006**, *40* (25), 4670–4678. https://doi.org/10.1016/j.atmosenv.2006.04.028.

(11) Delp, W. W.; Singer, B. C. Wildfire Smoke Adjustment Factors for Low-Cost and Professional PM2.5 Monitors with Optical Sensors. *Sensors* **2020**, *20* (13), 3683. https://doi.org/10.3390/s20133683.

(12) Barkjohn, K. K.; Holder, A. L.; Frederick, S. G.; Clements, A. L. Correction and Accuracy of PurpleAir PM2.5 Measurements for Extreme Wildfire Smoke. *Sensors* **2022**, *22* (24), 9669. https://doi.org/10.3390/s22249669.

(13) Holder, A. L.; Mebust, A. K.; Maghran, L. A.; McGown, M. R.; Stewart, K. E.; Vallano, D. M.; Elleman, R. A.; Baker, K. R. Field Evaluation of Low-Cost Particulate Matter Sensors for Measuring Wildfire Smoke. *Sensors* **2020**, *20* (17), 4796. https://doi.org/10.3390/s20174796.

(14) Duvall, R.; Clements, A.; Hagler, G. S. W.; Kamal, A.; Vasu Kilaru, L.; Goodman, L.; Frederick, S. G.; Johnson Barkjohn, K.; VonWald, I.; Greene, D.; Dye, T. *Performance Testing Protocols, Metrics, and Target Values for Fine Particulate Matter Air Sensors: Use in Ambient, Outdoor, Fixed Site, Non-Regulatory Supplemental and Informational Monitoring Applications*; EPA/600/R-20/280; U.S. EPA Office of Research and Development: Washington, DC, 2021.